Stabilization of NaCl-containing cuttings wastes in cement concrete by in situ formed mineral phases

Lev Filippov [a,*], Fabien Thomas [a], Inna Filippova [a], Jacques Yvon [a], Anne Morillon-Jeanmaire [b]

[a] *Laboratoire Environnement et Minéralurgie, Nancy Université-UMR 7569 CNRS, B.P.40, F-54501 Vandoeuvre-lès-Nancy, France*
[b] *Total, Environment Department, 24 cours Michelet-La Défense 10, F-92069, Paris La Défense Cedex, France*

ARTICLE INFO

ABSTRACT

Disposal of NaCl-containing cuttings is a major environmental concern due to the high solubility of chlorides. The present work aims at reducing the solubility of chloride by encapsulation in low permeability matrix as well as lowering its solubility by trapping into low-solubility phases.

Both the studied materials were cuttings from an oil-based mud in oil drillings containing about 50% of halite, and cuttings in water-based mud from gas drilling containing 90% of halite. A reduction in the amount of dissolved salt from 41 to 19% according to normalized leaching tests was obtained by addition of potassium ortho-phosphate in the mortar formula of oil-based cuttings, while the aluminium dihydrogeno-phosphate is even more efficient for the stabilization of water-based cuttings with a NaCl content of 90%.

Addition of ortho-phosphate leads to form a continuous and weakly soluble network in the cement matrix, which reduces the release of salt. The formed mineralogical phases were apatite and hydrocalumite. These phases encapsulate the salt grains within a network, thus lowering its interaction with water or/and trap chloride into low-solubility phases.

The tested approaches allow to develop a confinement process of NaCl-containing waste of various compositions that can be applied to wastes, whatever the salt content and the nature of the drilling fluids (water or oil).

© 2009 Elsevier B.V. All rights reserved.

1. Introduction

Drilling in saline geological formations turns out as a real environmental issue in areas where reject of alkaline chlorides cuttings is prohibited since they are considered as a major source of pollution in situations such as onshore drilling and drilling in protected areas. In marine areas, where the regulation applies the zero discharge policy of harmful components, the only option is to bring the cuttings back to shore for disposal. At present time, there is no efficient stabilization technique for NaCl or KCl containing cuttings.

A mineralogical and geochemical approach has been followed here, aiming at in situ formation of geomimetic materials covering the salt grains and/or trapping the chloride ions.

The most cost effective and reliable technique for immobilization of large amounts of wastes is the inclusion in a hydraulic binder based matrix, for example lime, pozzolanas, Portland or slag cement. The interest of such an approach is to bind chlorides in the concrete. Incidentally, the sodium and chloride ions affect the phase transformation in the cement paste during curing and hardening, as revealed by studies on the interaction of mortars with see water [1–3]. At high concentration, sodium chloride acts as a retarder and decreases the mechanical strength [4]. The addition of reagents with multivalent ions could improve the stability of the precipitates. Phosphate ions are excellent candidates for this purpose, since they can be introduced under the form of available hydrogeno-phosphates stable under pH 4 that will convert into apatitic materials when exposed to more alkaline media.

Many works were already dedicated to the use of ortho-phosphates in the field of the waste stabilization [5]. Associated or not with cement, they are used to immobilize and store low and intermediate-level radioactive wastes [6,7].

The effects of ortho-phosphate compounds reported in the literature are still a matter of controversy. On one hand, they are seen to be retarders of cement hydration [8,9]. Thus, the setting time can be strongly delayed whereas hardening can be greatly lowered at least at early ages. On the other hand, ortho-phosphate anions are described as setting accelerators and hardeners [10]. Moreover, according to Cau Dit Coumes and Courtois [11] and Bénard et al. [9,12], the presence of ortho-phosphate at high concentration ($>25\,\mathrm{g\,L^{-1}}$) in the waste appears to be very favorable since most fea-

tures of the resulting mortar were improved. The most important parameters for waste stabilization such as setting time and swelling during wet curing are decreased.

Phosphates can also be used for stabilization of mixed wastes such as ashes, cementing pastes, salts at low temperature [5]. The ability of phosphate ceramics to form at low temperature is of great interest, since volatile components such as chlorides, fluorides and heavy metals present in waste cannot be brought up to the usually high temperatures required in classical stabilization and solidification processes [13]. Nzihou et al. have developed a process of fly ash stabilization consisting in a chemical treatment with phosphate followed by a thermal treatment [14], leading to a pyromorphite-like compound. The evolution of rich in calcium and phosphates mixtures lead to precipitate apatite-like minerals at medium and elevated pH as shown in concretes [15].

Chloride-binding ability is also related to the formation of Friedel's salt [16,17]. One ambition of this work is to treat the chloride salt-containing cuttings with phosphates to limit or stop the salt diffusion, based on the formation of insoluble species by reaction of the mineral phases of the cuttings and of the cement with phosphates. This approach can be regarded as an encapsulation of the salt grains by a stable matrix, which traps one part of the chlorides and decreases the elements mobility.

2. Materials and methods

2.1. Studied samples

Two types of salt cuttings were studied (Table 1). The first sample, named "TFE", originated from an offshore drilling campaign. The drilling mud used here was based on a 95/5 water/oil emulsion. The recovered cuttings are separated on the field from the oil, by thermal desorption and stored as a pasty solid.

The second material, named "GDF", originating from an onshore drilling program in southern France, was almost pure NaCl. The water content determined from the dry weight and taking into account the salt content of the brine, was 23.3% (w/w).

2.2. Additives

Several additives were tested: Portland cement (CEM I 42.5N), quartz (0–1680, 0–140 or 140–1680 μm fractions), and hydrogenophosphate salts KH_2PO_4, $CaHPO_4$ and $Al(H_2PO_4)_3$. For the sake of simplicity the latter will be called "potassium, calcium and aluminium phosphate" all along this paper. Addition of quartz aimed at improving the cement setting and mainly occurs as an additive that acts as a mass diluting compound of the total salt content in the specimens, though, <5 μm quartz particles are subject to pozzolanic reactions [35].

2.3. Preparation of specimens

Mixtures of various proportions of cuttings, quartz, phosphates and cement were completed. Each addition of product was followed by mechanical blending for 1–3 min. Finally, the water was added at a ratio of water/cement 0.7–1.0 in order to obtain relatively fluid slurry, easy to pour in cylindrical molds (3.5 cm × 7.0 cm). The mortar specimens were aged for 1–70 days. The usual 28-day duration of setting before the leaching tests was considered for most specimens. The exact composition of specimens is presented in the section discussing the leaching tests results.

2.4. Leaching tests

The leaching tests were carried out according to the AFNOR X 31–211 (1994) procedure [18]. The solidified specimens were weighed and placed in hermetically closed, 2 L cylindrical polyethylene bottles. Deionised water was added at a solid/liquid ratio of 1/10. Permanent magnetic stirring was ensured at a rotation speed of 150 ± 30 rpm. To reach a free circulation of water around the specimens, the latter were placed on a 2.5 cm height metallic support.

The specimens and leaching solution were separated after 24 ± 0.5 h of leaching. After leaching, the samples were weighed and the sodium concentration in the leachate was measured by atomic absorption to recalculate the NaCl concentration. The use of sodium concentration to estimate the NaCl solubilisation or stabilization is based on the results reported in [3] using multinuclear magnetic resonance spectroscopy for determining the chloride fixation in the cement matrix and characterizing new phases appearing through the interaction of chloride with CSH phases. The results clearly state that sodium does not affect the hydration process, while chloride quickly disappears due to chemical reactions with the cement components. In fact, ^{35}Cl spectroscopy showed that only solid or adsorbed chloride is observed and that chloride ions are absent after drying [3].

The weight loss was $m\% = 100\,(m_0 - m_l)/m_0$, were m_0 and m_l are the sample weights before and after leaching.

The proportion of dissolved salt S (%) was calculated as the ratio of the amount of dissolved salt to the total salt content in the solidified cuttings, according to the following expression:

$$S = 100 \left(\frac{C_l(0.01 \cdot m_0)}{C_0(1 - H) \cdot P_{cut}} \right)$$

with C_l the concentration of salt (g/L) in the leaching solution, C_0 the salt content in the cuttings, H the water content of the sample, P_{cut} the amount of cuttings (g) incorporated in the solidified specimen.

The coefficient 0.01 accounts for the correction of units of measure according to the solid/liquid ratio in the leaching tests. The parameter S allows an estimation of the efficiency of the applied treatment and provides an accurate comparison of the stabilization results.

2.5. Analytical methods

In order to concentrate the secondary minerals for the purpose of analysis, the salt of the cuttings was dissolved in deionised water, during 1 h at a solid/liquid ratio of 1/10.

The crystalline phases were characterized by X-ray diffraction using a Bruker D8 Advance diffractometer operating with the Co $K\alpha_1$ radiation in reflection mode on disoriented powdered samples. Chemical analysis was performed using atomic absorption on a PerkinElmer AAnalyst 800 device. The local elemental composition was characterized using a scanning electron microscope Hitachi 2500 (unpolished broken proofs) and a CAMECA SX50 electron microprobe (kerosene polished section).

Table 1
Mineralogical composition of the studied cuttings.

Mineral	Formula	Content (%)	
		TFE	GDF
Halite	$NaCl$	60.7	89.8
Barite	$BaSO_4$	25.9	
Calcite	$CaCO_3$	3.5	
Magnesite + dolomite	$MgCO_3 + (Mg,Ca)(CO_3)_2$		2.4
Anhydrite	$CaSO_4$	3.4	2.5
Illite/Mica	$Al_2Si_3AlO_{10}(OH)_2K$	2.6	0.4
Quartz	SiO_2	1.6	1.3
Feldspars (K)	Si_3AlO_8K	0.7	1.2
Hematite	Fe_2O_3	0.5	
Total		98.9	97.6

Table 2
Composition of TFE cutting specimens and leaching results: the total solid mass (cutting + cement + quartz) = 108 g.

Sample	Additives			Curing time (days)	Weight loss, m (%)	Dissolved salt, S (%)
	Quartz (%)	Cement (%)	Phosphate[a] (g/kg cuttings)			
OK2	–	25	–	47	8.94	42.7
OK3	–	25	–	28	7.94	41.3
OK4	–	25	–	1	9.88	53.2
OK13	–	40	–	28	5.48	28.5
OK30	18.8	25	–	28	6.15	33.3
OK44	17.9	25	50.0 (K)[a]	20	3.08	19.0
OK57	17.9	25	50.0 (Ca)[b]	28	4.18	24.1

[a] $K–KH_2PO_4$.
[b] $Ca–Ca(H_2PO_4)_2$.

3. Results and discussion

3.1. Characteristics of the studied samples

The constitutive phases were identified and quantified by combining the results of X-ray diffraction, chemical analysis and electron microprobe. In both the cases, halite (NaCl) was the major component of the studied cuttings, respectively around 60% for TFE and 90% for GDF (Table 1).

However, the samples differ in their minor minerals. In this regard, the TFE sample contains essentially barite, and lower amounts of calcite, anhydrite and quartz. Clays are also present in the form of illite/mica, and probably of swelling clays as suggested by weak scattering in the 12–13 Å domain of the X-ray diffractograms. The GDF sample contains anhydrite, carbonates and a small proportion of illite/mica as minor minerals.

3.2. Leaching of the solidified specimens

The composition of the specimens and the results of the leaching experiments are presented and discussed separately for the two initial cutting samples TFE and GDF. The efficiency of various treatments is expressed as the percentage of dissolved salt according to the total amount of salt in the solidified cuttings.

3.2.1. TFE sample

For the specimens prepared without any phosphate addition the amount of released salt strongly depends on the duration of cement hydration (Table 2): a 1 day hydration results in 53.2% of salt release, whereas 28 and 47 days curing reduce the release to about 42%. The amount of added cement also influences the leaching results:

comparing runs OK3 and OK13, adding 40% of cement instead of 25% results in a strong decrease of the salt release from 41.3 to 28.5%.

However, the addition of cement only reduces the kinetics of salt dissolution, as revealed by the formation of salt crystals at the surface of the leached specimens after storage under ambient atmospheric conditions (Fig. 1a and b). A high proportion of cement decreases the pores size, which would result in the formation of salt filaments on the surface of the specimens (Fig. 1c), while the shape of salt crystals is cubic for the low cement proportion. Indeed, the salt of the cement matrix is in equilibrium with the saturated solution during cement setting. If the structure of mortar is porous, the gradient of the salt concentration between interstitial and condensed water favors the migration of salt towards the specimen surface where it crystallizes. The porosity of the solidified cuttings in the specimen is then of primary importance.

The addition of 25% of quartz (OK30) decreases the proportion of dissolved salt from 41.3 to 33.9%.

The treatment of the cuttings with potassium phosphate strongly decreases the amount of dissolved salt from 41.3 to 19.1% (Table 2, samples OK44 and OK57). Moreover, crystallization of salt on the surface of the specimens (Fig. 1d, OK44) was not observed. Using calcium phosphate also reduced the remobilization of the salt ($S = 24.1\%$), but with a lower efficiency than the use of potassium phosphate.

3.2.2. GDF sample

The GDF sample contains almost pure NaCl. Therefore, the salt content in the specimens was higher than in the TFE specimens for similar operating conditions. Therefore, the setting of mortar required higher amounts of cement and quartz which confer a structural skeleton to the whole, the addition of quartz was empiri-

(a) OK3 **(a) OK30** **(b) OK13** **(c) OK44**
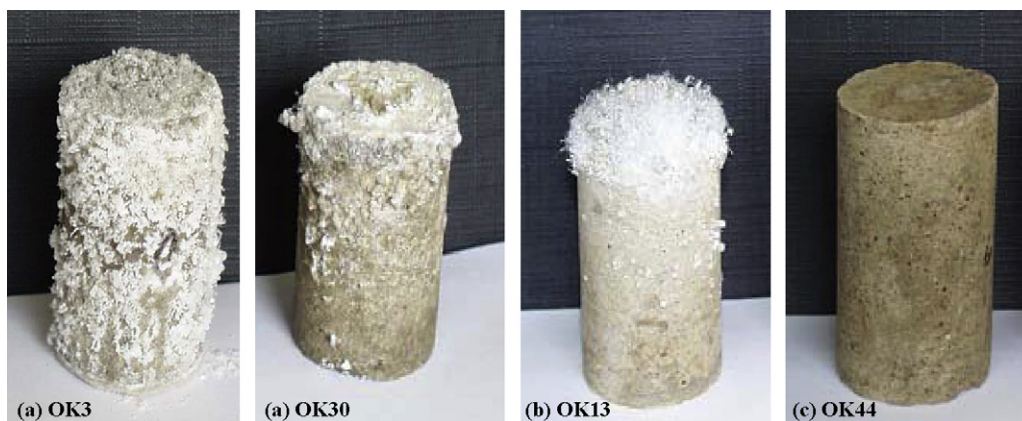
Fig. 1. Influence of mortar composition (see Table 2) on the salt crystallization on the surface of leached specimens after contact with atmosphere for 3 months. The gradient of the salt concentration between interstitial and condensed water favors the migration of salt towards the specimen surface where it crystallizes (a and b). The addition of high proportion of cement (c) only reduces the pore sizes and favors the growing of filament-like halite crystals. Salt crystallization is not observed when phosphate was added in the cement past (d).

Table 3
Composition of GDF cutting specimens and leaching results: the total solid mass (cutting + cement + quartz) = 105 g: quartz size fraction 0–1680 μm.

Sample	Additives			Curing time (days)			
	Quartz (%)	Cement (%)	Phosphate[a] (g/kg cuttings)	28		70	
				m (%)	S (%)%	m (%)	S (%)
G1[b]	37.5	24.8		7.42	52.5		
G2[c]	37.5	24.8	–	7.19	48.1		
G3	37.5	24.8	–	6.32	41.4	4.95	33.0
G8	25.5	35.0	–	6.08	33.7	3.82	28.9
G9	20.9	40.0	–	4.02	31.0	3.32	32.1
GP2	37.5	24.8	52.5 (K)[a]	5.09	27.8	3.10	20.9
GP18	31.7	30.0	52.5 (K)[a]	3.35	28.2	3.31	24.6
GP19	25.5	35.0	52.5 (K)[a]	2.43	25.9	3.15	21.7
GP11	37.5	24.8	50.0 (Al)[a]	3.12	14.8	2.48	14.7
GP12	37.5	24.8	30.0 (Al)[a]	3.49	23.9	2.65	19.2
GP13[b]	37.5	24.8	50.0 (Al)[a]	1.66	13.7	2.04	12.7

[a] K, KH_2PO_4; Al, $Al(H_2PO_4)_3$.

[b] Size fraction of quartz is 0–140 μm.

[c] Size fraction of quartz is 140–1680 μm.

cally adjusted through the normative rules, without measuring the setting time. A special attention was also drawn to the curing time, by comparing the dissolved salt proportion after 28 or 65–70 days.

Without phosphate addition, the salt release during the leaching tests shows the same behaviour as for the TFE sample. The proportion of dissolved salt S is high, ranging from 31 to 52.5% for a total cement plus quartz proportion close to 60%. The values of weight loss and dissolved salt decreased when the cement proportion in the mortar increased from 25 to 40% (Table 3, samples G2, G3 and G9).

The treatment of cuttings with potassium phosphate resulted in a better stabilization of the GDF cuttings, since the amount of dissolved salt dropped down to 26–28% for the same composition of mortars (see G3 and GP2, G7 and GP18, G8 and G19 in Table 3). However, these results cannot be considered as satisfactory due to the high salt content of the leaching solution (32.8% maximum decrease for G3 and GP2), though a relatively high amount of phosphate was used. It can be underlined that the effect of phosphate is proportional to the amount introduced in the specimen formulation.

The action of aluminium phosphate was much more significant than that of potassium phosphate. The proportion of dissolved salt is divided by 2.7 for the coarser size fraction of quartz in the mortar formula (Table 3, G3 and CP11) or by 3.9 for the finer size fraction (Table 2, G1 and GP13) with 50 g/kg of aluminium phosphate applied.

The efficiency of phosphates for the salt stabilization suggests the formation of a mineralogical barrier limiting the salt diffusion during the cement setting and later, upon leaching of solidified specimens and during contact with ambient atmosphere. Such a barrier results from the interaction between the salt, the phosphate and the cement components. Therefore, the duration of the cement setting may influence the stabilization effectiveness. In order to

check this hypothesis, two sets of the specimens from GDF cuttings were manufactured, one leached after 28 days of curing and the other one after 70 days. The parameters m and S systematically are lower for the phosphate treated samples after a 70 days curing compared to those after a 28 days (Table 3). The decrease was strongest and reached 10% when potassium phosphate was used. Aluminium phosphate generated lower decrease according to curing time, but showed the best effectiveness independently of the curing time (Table 3, samples GP11, GP12, GP13).

For the non-treated GDF cuttings, the proportion of dissolved salt randomly varies with curing time. The value of S decreases for the specimens with a high content of cement (G8), while the behaviour of the other samples of this series does not relate to their compositions, showing generally a decrease of the weight loss and dissolved salt proportion.

It must be noted that the size fraction of quartz 0–1680 μm is very convenient for the present use, and that a finer fraction (0–140 μm) did not improve the stabilization, which indicates that, in this range of silica particle size variation, the production of secondary CSH through pozzolanic reactions is not effective.

3.3. Mineralogical transformations

3.3.1. Mineral composition of specimens

The above leaching tests clearly show the cumulative effect of cement and phosphates on the stabilization of salt cuttings, and suggest that one or more insoluble phases precipitate in the phosphate treated samples. SEM examination of the OK44 specimen shows that after 3 months, the salt appears as an amorphous gel-like phase rather than as cubic crystals (Figs. 2a and 3b). However, the phosphate is still uniformly distributed in the cement phase, without concentration at the salt–cement interface (Fig. 2b and c).

Fig. 2. SEM pictures of the OK44 specimen: (a) cement matrix, (b) distribution of Na, and (c) distribution of P.
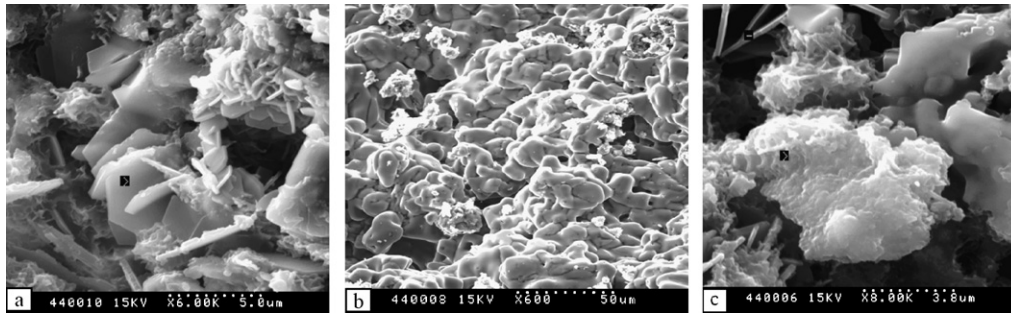
Fig. 3. Neoformed phases in the cement matrix with phosphate addition (sample OK44): (a) platelets of hydrocalumite, (b) amorphous aspect of NaCl, and (c) main aspect of cement matrix.

SEM images (Fig. 3) clearly show connections between the phases of the matrix, suggesting the presence of a continuous network of neoformed phases. Detailed analysis of this network reveals hexagonal platelets (Fig. 3a). The atomic composition of these platelets from EDS analysis corresponds to the chemical composition $Ca_{4.47}Al_2Cl_{2.19}Si_{0.52}O_{19.7}$ (Fig. 4), which is close to that of an hydrated hydrocalumite $Ca_4Al_2Cl_2O_7 \cdot 12(H_2O)$ [19]. If the presence of Si is attributed to a contamination of the local EDS analysis by silicates, the calculation of the formula yields the composition of Friedel's salt.

EDS analysis of the cement matrix at different spots do not allow the calculation of the phase formula in such a complex media. However, the following remarks can be made: the systematic presence of phosphorous (Fig. 3c, Fig. 5) suggests that the phosphate phases are formed in these conditions, though no evidence for such minerals is brought by SEM observations. Various local EDS elemental analyses shown the presence in cement matrix the amorphous phases containing of phosphorus.

The extraction of Cl^- from NaCl upon formation of hydrocalumite would explain the aspect change of the salt phase in the cement matrix, since partial dissolution results in rounded, molten shape (Figs. 2a and 3b).

Finally, sulphur was detected on the specimens, but surprisingly not correlated with barium, although the initial cutting samples contained barite. Thus formation of ettringite can be suggested from SEM and EDS results with its characteristic sticky morphology (Fig. 3c).

3.3.2. Formation of hydrocalumite

The presence of hydrocalumite is confirmed by the characteristic XRD peaks (Fig. 6) of β-hydrocalumite at 7.78, 3.88 and 3.76 Å (sheet 35–105, JCPDS file, 1985).

Chloride trapping in hydrocalumite in the ordinary Portland cement matrix has been reported by several authors [20–22]. Indeed, at the high pH of the pore solution, the dominant aluminium species is aluminate, and hydrocalumite precipitates according to the following reaction, that requires protons [23,24]:

$$2Ca(OH)_2 + Al(OH)_4^- + Cl^- + 2H^+ + H_2O$$
$$\rightarrow Ca_2Al(OH)_6Cl \cdot 3H_2O \tag{1}$$
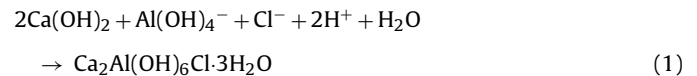
It can be surprising that hydrocalumite was detected here by XRD, since previous studies have shown that it can only be identified by this technique when it forms from $CaCl_2$ [17], or inferred from DTA/TG measurements [25]. The point is that the major XRD peak of hydrocalumite at 7.81 Å can be mistaken for the major peak of a C3A hydrate at 8.0 Å. Thus, the identification of Friedel's salt in this study was stated if the triplet of this phase (7.78, 3.88 and 3.76 Å) were clearly identified on the diffractograms. Indeed, in the present work, hydrocalumite was not detected on specimens that were not treated with phosphates (Fig. 8a). Only specimens treated with phosphates showed the typical XRD peak of hydrocalumite at 7.82 Å. This observation supports the assumption that the formation of hydrocalumite and the transformation of added phosphate are mechanistically correlated.
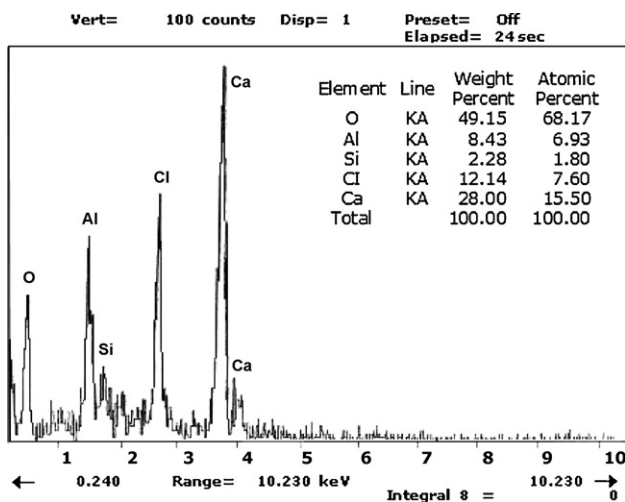

Fig. 4. SEM-EDS spectrum and elemental analyses of hexagonal platelets observed in the cement matrix of specimen OK44 with potassium phosphate (see Fig. 3a). The reconstituted formula of this phase corresponds to the chemical composition $Ca_4Al_2Cl_2O_6(H_2O)_{12}$ which is close to that of hydrocalumite.
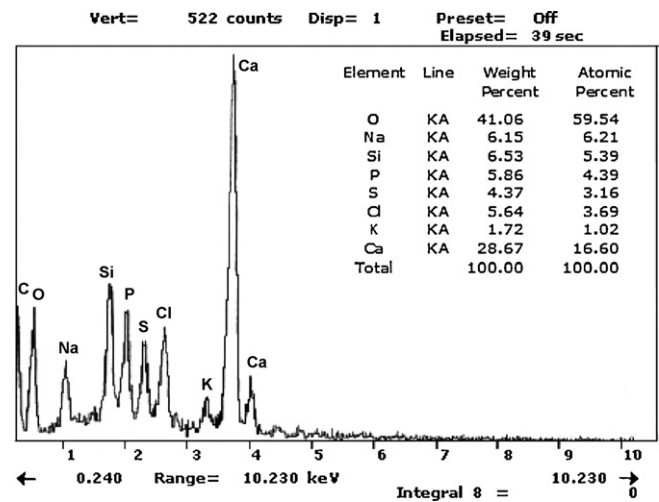

Fig. 5. SEM-EDS spectrum and elemental analyses pointed in the cement matrix of specimen OK44 with potassium phosphate (see Fig. 3c). The analysis of the cement matrix at different spots does not allow the calculation of the phase formula. The observations reveal the existence of various amorphous phases containing phosphorus and Ca.
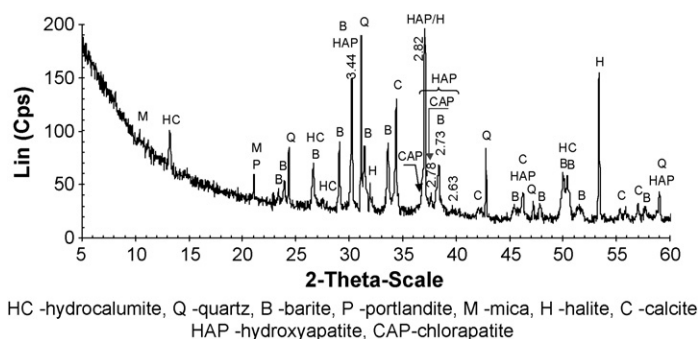
Fig. 6. Hydrocalumite and apatite identification from XRD diffractograms of specimen OK44 aged for 3 months.

3.3.3. Formation of hydroxyapatite

Phosphorous is almost evenly distributed over the cement matrix as shown by SEM-EDS (Fig. 3c, Fig. 5). Although no individualized phosphate bearing particles were observed on the micrographs, hydroxyapatite was identified on the X-ray diffractograms by its characteristic peaks at 2.77–2.78 Å and by the shoulders at 2.84 Å and at 2.73 Å (Fig. 6), beneath the very intense peaks of halite at 2.82 Å, barite at 2.70 Å and calcite at 3.03 Å. Apatite peaks appeared only after at least 3 months ageing (P44) or even 1 year as for the specimen OK44 in the Fig. 7. The chlorapatite was well identified from the peak at 2.78 Å and at 2.73 Å without overlapping by the barite peaks.

The intensity of the peak at 2.83 Å for barite is higher of that for 2.73 Å. The report of the intensities is reversed on the diffractograms sample OK44 (Fig. 7): the increase of the intensity of peak at 2.73 Å confirms the hydroxyapatite crystallization and reveals the phosphate compounds transformation and apatite crystallization as a function of specimen ageing. Moreover, the disappearing of the peak of halite at 2.82 Å on the diffractograms of specimen OK44 (Fig. 7) may indicate the profound transformation of halite structure in the mortar and agrees with aspect changes of NaCl crystals observed on the Figs. 2a and 3b.

The transformation of phosphate at strongly alkaline pH is well documented in pure systems. Ortho-phosphate reacts with Ca^{2+} ions to form hydroxyapatite (HAP) $Ca_5(PO_4)_4(OH)$ via a number of possible intermediate metastable phases such as tricalcium phosphate (TCP) $Ca_3(PO_4)_2$, dicalcium phosphate dihydrate DCPD, octacalcium phosphate (OCP) $Ca_8H_2(PO_4)_6 \cdot 5H_2O$ [26,27]. It was already shown that hydrolysis of hydrated dicalcium phosphate $CaHPO_4 \cdot 2H_2O$ and ageing of these crystals at 25 °C for 3 months leads to OCP [28,29], considered as a precursor of HAP [26]. These observations support the assumption that in conditions similar to those of this work, neoformed phosphate phases such as OCP can readily precipitate in the cement paste after mixing when phosphate ions are added. The SEM-EDS allow to conclude that such assumption on the existence of amorphous phases can be justified with observations and measures on the specimens treated with phosphate (see Fig. 3c, Fig. 5). Indeed, the wide region of 2θ from 3 to

20 in diffractogram of Fig. 6 confirms the evidence of a high proportion of poor crystallized or/and amorphous phases which disappear in the diffractograms of the same specimen analyzed after 1 year ageing (Fig. 7).

Then, after the transition from OCP to HAP at low temperature occurs through a metastable amorphous calcium phosphate phase (ACP) which is less soluble than the medium is more basic and rich in Ca^{2+} [30], and which was probably observed in the present study among the many amorphous species revealed by SEM, because its formation is strongly favored in these conditions (Figs. 3c and 5).

Therefore HAP is likely to form under the present conditions, according to the following pathway:

$$DCPD \rightarrow OCP$$

$$OCP + 2Ca^{2+} \rightarrow HAP + 3H_2O + 4H^+ \tag{2}$$
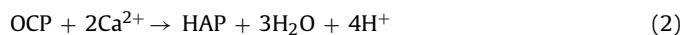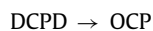
The same mechanism of OCP to HAP transformation was suggested in recent work by Bénard et al. [9] considering a decrease in volume fraction of the solid phase by a factor 1.4, as calculated from the measured densities of the phosphate compounds, and based on the thermodynamic calculations of Boskey and Posner [31].

The Na^+ and K^+ ions would not have any influence on the crystallization of HAP. According to Brown and Chow one would obtain a mixture of HAP and OCP as a function of the Ca/P molar ratio [30].

3.4. Mechanism of chloride trapping in neoformed phases

The most important conclusion from above discussion consists in relation between hydrocalumite and apatite formation in the solidified specimen aged for certain period.

The reaction (2) results in an acidification of the pore solution with the increase in the proportion of $Ca(OH)_2(aq)$, which is required for the reaction (1) to produce hydrocalumite.

The relation between crystallization of HC and that of HAP is confirmed by the disappearing of XRD reflections of portlandite in the diffractograms of the specimen G3, accompanied by a subsequent increase of the intensity of hydrocalumite peaks on the XRD pattern of specimens GP11 from GDF cuttings containing phosphate (Fig. 8).

The addition of aluminium phosphate in the cement paste allows the most efficient stabilization of salt as shown by the results of leaching tests on the specimens GP11–GP13 (Table 3). The available aluminium favors the formation of Friedel's salt as was shown for the stabilization of aluminium refining wastes [19] and for the stabilization of salt-containing wastes in the Portland cement matrix [32].

Summarizing, chloride binding from NaCl in hydrocalumite can be explained by the following reaction:
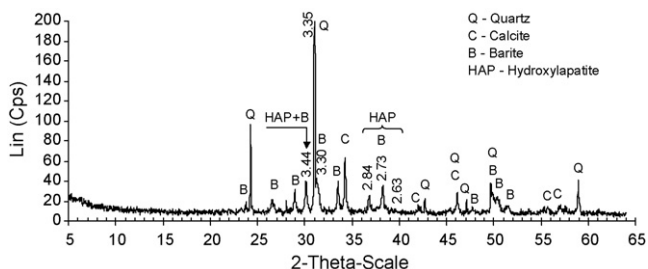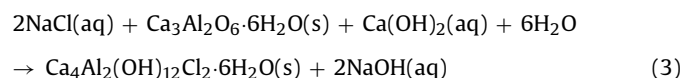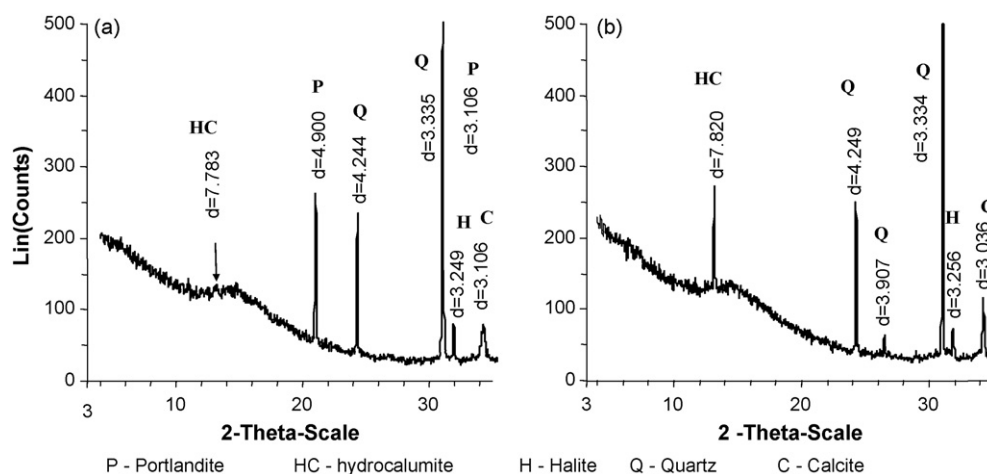
$$2NaCl(aq) + Ca_3Al_2O_6 \cdot 6H_2O(s) + Ca(OH)_2(aq) + 6H_2O$$

$$\rightarrow Ca_4Al_2(OH)_{12}Cl_2 \cdot 6H_2O(s) + 2NaOH(aq) \tag{3}$$

Fig. 7. XRD diffractograms of specimen OK44 aged for 1 year.

Fig. 8. XRD diffractograms showing portlandite (P) to hydrocalumite (HC) transition in mortar with addition of Al phosphate in the specimens from GDF cuttings: (a) specimen G3 with no phosphate; (b) specimen GP11 with phosphate of Al.

This reaction shows an alkalinisation of the pore solution, which decreases the solubility of $Ca(OH)_2$ slowing down the whole process. This process is counteracted by the release of protons upon formation of hydroxyapatite. Thus, the mechanism proposed for NaCl stabilization consists in chloride trapping in the HC supported by the formation of HAP when phosphates were added. Due to the fact that the formed protons will be consumed in the limit of availability of calcium hydroxide and will not affect the pH: they only favors an increase of the proportion of Ca^{2+}. Thus, the protons liberation during OCP to HAP transformation accelerates the kinetics of reaction 3.

Another way to favor reaction (3) could be the transformation of the added aluminium phosphate into calcium aluminate by reaction with portlandite. This was confirmed in the test with GDF samples when the Al phosphate addition is more efficient for chloride trapping in the solidified specimens.

Nevertheless, a global mechanism of destabilization appears to be pH-dependent: Friedel's salt dissolves at 20 °C generating a pH value of 12. Among the factors, which can decrease the pH of the concrete pore solution, are carbonation and pozzolanic materials additions that consumes the excess of portlandite [33]. In this sense, Suryavanshi and Swamy noted that carbonation of Portland concrete resulted in dissolution of Friedel's salt [34]. Goni and Guerrero review's stated that the solubility of Friedel's salt increased in Portland cements blended with silica fume, as the alkalinity of the pore solution dropped strongly as free chloride increased, due to the pozzolanic reaction of silica fume with calcium hydroxide [33]. In fact, the Friedel's salt stay stable in the limit of consumption of portlandite.

We observe that the ageing and exposure of specimen OK44 to atmosphere favor the destabilization of hydrocalumite as show the diffractograms presented in Fig. 7 with accentuation of hydroxyapatite and chlorapatite reflections. In fact the intensity of peak at 2.83 Å in comparison to the intensity of peak at 2.73 Å shows a considerable increase in the proportion of well crystallized hydroxyapatite.

The availability of chloride in the pore solution allows the formation of chlorapatite and hydroxyapatite, which were supposed, here, to be formed in the solidified cutting specimens. The new-formed phases, during cement setting and ageing of the mortar, trap chlorides in the stable compounds and explain the effectiveness of NaCl stabilization in the cement matrix where the phosphates are used as additives.

4. Conclusions

Cumulative effect of cement and phosphates allows an efficient trapping of chloride in a cement matrix due to the development of stable and insoluble phases at the salt–cement boundary. A reduction in the amount of dissolved salt from 41 to 19% during normalized leaching tests was obtained by addition of potassium phosphate in the mortar formula of oily-based cuttings, while the aluminium phosphate is more efficient for the stabilization of water-based cuttings with a salt content of 90%.

The study of the specimens obtained from salt cutting revealed an evolution of the mineralogical composition during maturation. The two most interesting aspects are on one hand the good dispersion of phosphate on the surface of the salt grains and on the other hand the formation of Fridel's salt and hydroxyapatite under the conditions of pH and Ca content brought by cement. Thus, doping cement matrix with phosphates constitutes a promising way of stabilization if the time of curing is rather long. At short times, the filling of intergranular spaces by aluminium or potassium phosphate and cement slows down the dissolution of salt; at longer times the low-solubility apatite phases gradually develop.

Hydrocalumite was detected on the diffractograms after 28 days of solidification, while apatite appeared only in the specimens cured at least 3 months (from Oil based cuttings) or even 1 year (from Water based cuttings). In the latter case, hydroxyapatite and chlorapatite was well identified from XRD spectrum.

The development of apatite phases from amorphous phosphate phases accompanied by the acidification of pore solution may be supposed as a major factor for chloride binding in the cement due to creation of favorable conditions for hydrocalumite crystallization.

References

[1] A. Delagrave, M. Pigeon, J. Marchand, E. Revertegat, Influence of chloride ions and pH level on the durability of high performance cement pastes (Part II), Cem. Concr. Res. 24 (1994) 1433–1443.
[2] A. Delagrave, M. Pigeon, J. Marchand, E. Revertegat, Influence of chloride ions and pH level on the durability of high performance cement pastes (Part IV), Cem. Concr. Res. 26 (1996) 749–760.
[3] F. Barberon, V. Baroghel-Bouny, H. Zanni, B. Bresson, J.-B. d'Espinose de la Caillerie, L. Malosse, Z. Gan, Interactions between chloride and cement-paste materials, Magn. Reson. Imag. 23 (2005) 267–272.
[4] A.R. Brough, M. Holloway, J. Sykes, A. Atkinson, Sodium silicate-based alkali-activated slag mortars, Part II. The retarding effect of additions of sodium chloride or malic acid, Cem. Concr. Res. 30 (2000) 1375–1379.

[5] J.R. Conner, S.L. Hoeffner, The history of stabilization/solidification technology, Crit. Rev. Environ. Sci. Technol. 28 (1998) 325–396.

[6] A. Wagh, S.R. Strain, S.Y. Jeong, D. Reed, T. Krause, D. Singh, Stabilization of rocky flats Pu-contaminated ash within chemically bonded phosphate, J. Nucl. Mater. 265 (1999) 295–307.

[7] E.H. Oelkers, J.M. Montel, Phosphates and nuclear waste storage, Elements 4 (2008) 113–116.

[8] L. Ben-Dor, Y. Rubinsztain, The influence of phosphate on the hydration of cement minerals studied by DTA and TG, Thermochim. Acta 30 (1979) 9–14.

[9] P. Bénard, S. Garrault, A. Nonat, C. Cau Dit Coumes, Hydration process and rheological properties of cement pastes modified by orthophosphate addition, J. Eur. Ceram. Soc. 25 (2005) 1877–1883.

[10] J.M. Casabonne-Masonnave, Immobilization of borates and phosphates anions with saturated lime solutions, Solid State Ionics 59 (1993) 133–139.

[11] C. Cau Dit Coumes, S. Courtois, Cementation of a low-level radioactive waste of complex chemistry—investigation of the combined action of borate, chloride, sulfate and phosphate on cement hydration using response surface methodology, Cem. Concr. Res. 33 (2003) 305–316.

[12] P. Bénard, C. Cau Dit Coumes, S. Garrault, A. Nonat, S. Courtois, Dimensional stability under wet curing of mortars containing high amounts of nitrates and phosphates, Cem. Concr. Res. 38 (2008) 1181–1189.

[13] D. Singh, A.S. Wagh, J.C. Cunnane, J.L. Mayberry, Chemically bonded phosphate ceramics for *low-level* mixed-*waste* stabilization, J. Environ. Sci. Health Part. A: Environ. Sci. Eng. 32 (1997) 527–541.

[14] A. Nzihou, P. Sharrock, Extraction of chloride from fly ash and stabilisation of the residues by a hydroxylapatite sol-gel process, in: J. Mehu, G. Kesk, A. Navarro (Eds.), Proceedings of Waste Stabilisation End Environment, Lyon-Villeurbanne, April 13–16, v. 3, 1999, pp. 295–307.

[15] W. Ma, P.W. Brown, Effect of phosphate additions on the hydration of Portland cement, Adv. Cem. Res. 21 (1994) 1–12.

[16] A.K. Suryavanshi, J.D. Scantlebury, S.B. Lyon, Mechanism of Friedel's salt formation in cements rich in tri-calcium aluminate, Cem. Concr. Res. 26 (1996) 717–727.

[17] A. Delagrave, J. Marchand, J.-P. Ollivier, S. Julien, K. Hazrati, Chloride binding capacity of various hydrated cement paste systems, Adv. Cem. Based Mater. 6 (1997) 28–35.

[18] AFNOR, NF X 31–212, Essai de lessivage d'un déchet solide initialement massif ou généré par un procédé de solidification. Norme Française, 13 pp., 1994.

[19] F. Puertas, M.T. Blanco-Varela, T. Vazquez, Behaviour of cement mortars containing an industrial waste from aluminium refining. Stability in Ca(OH)$_2$ solutions, Cem. Concr. Res. 29 (1999) 1673–1680.

[20] J. Tritthart, Chloride binding in cement II. The influence of the hydroxide concentration in the pore solution of hardened cement paste on chloride binding, Cem. Concr. Res. 19 (1989) 683–691.

[21] C. Arya, N.R. Buenfeld, J.R. Newman, Factors influencing chloride-binding in concrete, Cem. Concr. Res. 20 (1990) 291–300.

[22] M.N. Haque, O.A. Kayyali, Free and water soluble chloride in concrete, Cem. Concr. Res. 25 (1995) 531–542.

[23] J. Yvon, D. Antenucci, E.A. Jdid, G. Lorenzi, V. Dutré, D. Leclerq, P. Nielsen, M. Veschkens, Long term stability in landfills of Municipal Solid Waste Incineration (MSWI) fly ashes solidified/stabilized by hydraulic binders, J. Geochem. Explor. 90 (2006) 143–155.

[24] J. Yvon, D. Antenucci, E.A. Jdid, G. Lorenzi, V. Dutré, D. Leclerq, P. Nielsen, Solidified/stabilized municipal solid waste incineration fly ashes in cementitious matrix: aluminium hydrolysis effect upon lead speciation in solids, In: Ernest C. Lehmann (Ed.), Landfill Research Focus, Nova Publishers, ISBN 1-60021-775-3 (Chapter 10), 2008, pp. 293–310.

[25] R. Luo, Y. Cai, C. Wang, X. Huang, Study of chloride binding and diffusion in GGBS concrete, Cem. Concr. Res. 33 (2003) 1–7.

[26] D.G.A. Nelson, H. Salimi, G.H. Nancollas, Octacalcium phosphate and apatite overgrowths: a crystallographic and kinetic study, J. Colloid Interface Sci. 110 (1986) 32–39.

[27] J.C. Heughebaert, G.H. Nancollas, The kinetics of crystallization ofoctacalcium phosphate, J. Phys. Chem. 88 (1984) 2478.

[28] J.C. Heughebaert, G.H. Nancollas, The growth of dicalcium phosphate dihydrate on octacalcium phosphate at 25 °C, J. Cryst. Growth 76 (1986) 192–198.

[29] J. Puech, J.C. Heughebaert, G. Montel, A new mode of growing apatite crystallites, J. Cryst. Growth 56 (1982) 20–25.

[30] W.E. Brown, L.C. Chow, Thermodynamics of apatite crystal growth and dissolution, J. Cryst. Growth 53 (1981) 31–41.

[31] A.L. Boskey, A.S. Posner, Conversion of amorphous calcium phosphate to microcrystalline hydroxyapatite: a pH-dependent, solution-mediated, solid–solid conversion, J. Phys. Chem. 77 (1973) 2313–2317.

[32] P.G. Malone, T.S. Poole, L.D. Wakeley, J.P. Burkes, Salt related expansion reactions in Portland cement-based wasteforms, J. Hazard. Mater. 52 (1997) 237–246.

[33] S. Goni, A. Guerrero, Accelerated carbonation of Friedel's salt in calcium aluminate cement paste, Cem. Concr. Res. 33 (2003) 21–26.

[34] A.K. Suryavanshi, R.N. Swamy, Stability of Friedel's salt in carbonated concrete structural elements, Cem. Concr. Res. 26 (1996) 729–741.

[35] J.C. Benezet, A. Benhassaine, The influence of particle size on the pozzolanic reactivity of quartz powder, Powder Technol. 103 (1999) 26–29.